Molecular dynamics simulation of the initiation of plastic deformation in nanocrystalline material

Takuya Uehara

Department of Mechanical Systems Engineering, Yamagata University, Japan
Corresponding author: uehara@yz.yamagata-u.ac.jp

Abstract

Molecular dynamics simulations were carried out to investigate the initiation mechanism of the plastic deformation in nanocrystalline material. A polycrystalline model consisting of four grains each of which had nano-meter order size was prepared. All atoms were arranged on the face-centered cubic lattice and rotated around the [001] axis keeping the (001) face on the *x*-*y* plane. The rotation angles were set different in every grain so that the grain boundaries were formed. Then an external compressive load was imposed at a constant rate until a plastic deformation was observed apparently. Several models were prepared by varying the combination of the crystal orientations of the grains, and the change in the configuration of atoms and variation of the stress as well as their dependency on the model were investigated. Common to all models, the stress increased monotonously in the early stage, when the atomic configuration sustains the initial state. Then an abrupt drop in stress was observed. At this moment, linear or planar defects were generated, and the initiation sites were inferred on the grain boundaries. It also revealed that a plateau was observed around the stress peak when a linear defect was generated, while the peak was sharp when a planar defect was generated.

Keywords: Molecular dynamics, Plastic deformation, Dislocation, Yielding, Computer simulation

Introduction

Microstructure of a metallic material strongly affects the macroscopic properties of the material, and, for instance, the strength of polycrystalline material increases as the grain size becomes smaller. Therefore, great efforts have been devoted to refining the crystal grains, and several types of methods, such as equal-channel angular pressing (ECAP), accumulative roll bonding (ARB), and asymmetric rolling methods, have been successfully developed [1-3]. As a result of this kind of severe plastic deformation (SPD) processes, the grain size of the material falls in the submicron order, and such materials are generally termed nanocrystals. The mechanical behaviors of these materials show a characteristic tendency due to relatively higher occupancy of the grain-boundary area, and especially the plastic behavior is significantly affected. To clarify the deformation mechanism in nanocrystalline materials, an atomistic investigation is necessary, and the molecular dynamics (MD) simulation is a quite effective tool for this purpose. To date, various kinds of simulations have been demonstrated, including generation of dislocation, restructuring and migration of grain boundaries, interaction between dislocation and grain boundaries, as well as grain refining or coarsening due to mechanical loading or thermal activation [4-6]. The author also has demonstrated various simulations on the plasticity including grain-boundary migration [7], deformation of polycrystalline shape-memory alloy [8], and transformation-induced plasticity [9]. However, comprehensive understanding and construction of unified theory on the nano-scale deformation are still difficult due to the complexity of the nanocrystalline material. For

example, in relatively large scale, the grain boundary energy is often represented as a function of the misorientation angle, but the grain-boundary energy is actually different if the atomistic structure is different even though the misorientation angle is the same. Therefore, a systematic investigation using a simple model, instead of realistic large model, is considered effective to achieve the goal. The author has demonstrated MD simulations on a severe tensile or compressive deformation process of a polycrystalline material. In our previous report [10-12], change in microstructure was focused, and the grain refinement was successfully observed. In this study, the focus is concentrated on the initiation of the plastic deformation based on a similar polycrystalline model. Defects in a grain as well as their initiation and motion were made visible using the potential energy so that plastic behavior is clearly shown.

Fundamental Equations

Classical molecular dynamics method is applied in this study. The fundamental equation is the following.

$$\ddot{\boldsymbol{r}}_i = \frac{1}{m_i}\boldsymbol{F}_i = \frac{1}{m_i}\sum_j \boldsymbol{f}_{ij}, \quad \boldsymbol{f}_{ij} = -\frac{d\phi}{dr}\frac{\boldsymbol{r}_{ij}}{|\boldsymbol{r}_{ij}|} \tag{1}$$

Here, $\boldsymbol{r}_i$ and m_i are the position vector and the mass of the i-th atom, and $\boldsymbol{F}_i$ is the force acting on the i-th atom. In addition, $\boldsymbol{F}_i$ is assumed to be represented by the summation of the two-body interatomic force $\boldsymbol{f}_{ij}$ and the force is represented by a two-body interatomic potential energy ϕ. As a representative form for a face-centered-cubic (fcc) crystal, the following Lennard-Jones-type function is applied.

$$\phi = 4D\left((R/r)^{12} - (R/r)^{6}\right) \tag{2}$$

Here, D and R are the material parameters in the dimension of energy and length, respectively, while they are diminished in a non-dimensional form. In this paper, all physical parameters and variables are represented in the dimensionless values.

Simulation Model

Figure 1 represents the simulation model. Two types of nanocrystalline models consisting of four grains are prepared. A pair of grains is arranged perpendicular to the external load in Type A, while they are arranged parallel to the load in Type B. Periodic boundary conditions are imposed in the all directions; accordingly, Grain 3 separated in Fig. 1 is actually a single grain domain. The thickness of the model is five unit cells without any grain boundary. The atoms are set on the lattice points of the fcc structure so that the (001) plane is on the x-y

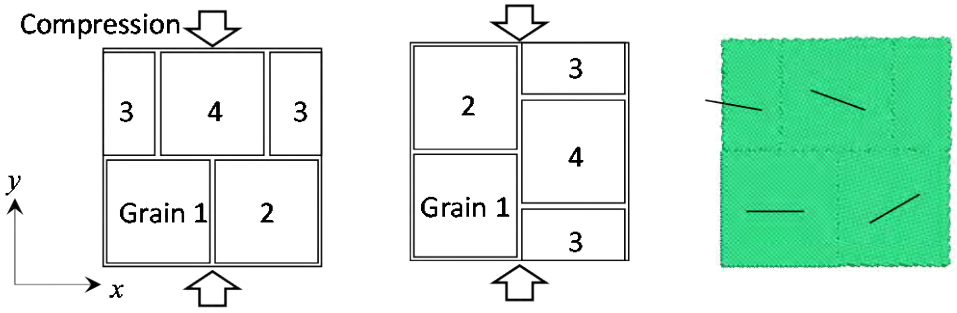

(a) Model A (b) Model B (c) Atomic configuration

Fig. 1.Illustration of the simulation model.

plane and the [100] direction to be the x axis. Then the crystal is rotated around the z-axis, where the rotation angles θ_k of the k-th grain are set distinctively.

Simulation Conditions

Table 1. Rotation angles in each grain.

Model ID	Grain No 1	2	3	4
z1	0	30	-10	-20
z2	0	-20	30	-10
z3	0	-10	-20	30

The combination of the rotation angles of the four grains is set variously, and the three cases shown in Table 1 are presented in this paper. Each simulation model is identified by the symbol combined with the type of grain arrangement, A or B; e.g. Model Az1. Fig. 1 (c) represents the initial configuration of atoms for Model Az1, where short lines drawn in every grain show the [100] orientation. A significant irregularity is induced at the grain-boundary area by this operation, and the 15000 time-steps are devoted for relaxation of the arrangement. Then an external compression is imposed by reducing the length in the y-direction L_y of the model at a constant rate. Then the average normal components of the stress in the lateral directions, x and z, are kept constant at zero by adjusting the edge length L_x and L_z. The compression rate is set as ΔL_y = 1.0 per 8000 time steps (L_y is approximately 73.0 for all models).

Simulation Results --- Model Az1

Simulation result for Model Az1 is shown in Fig. 2, which represents the variation of configuration of atoms during compressive deformation process. The color indicates the potential energy of each atom, where red and blue represent the maximum and minimum values, respectively, and the intermediate colors are continuously allocated. Accordingly, grain boundaries are depicted in green or yellow.

Figure 2(a) exhibits the configuration of atoms at the beginning of loading after relaxation. Every grain maintains the original shape of square, though the top-right grain boundary between Grains 3 and 4 is rather curved. Overall, no specific change in grain arrangement and

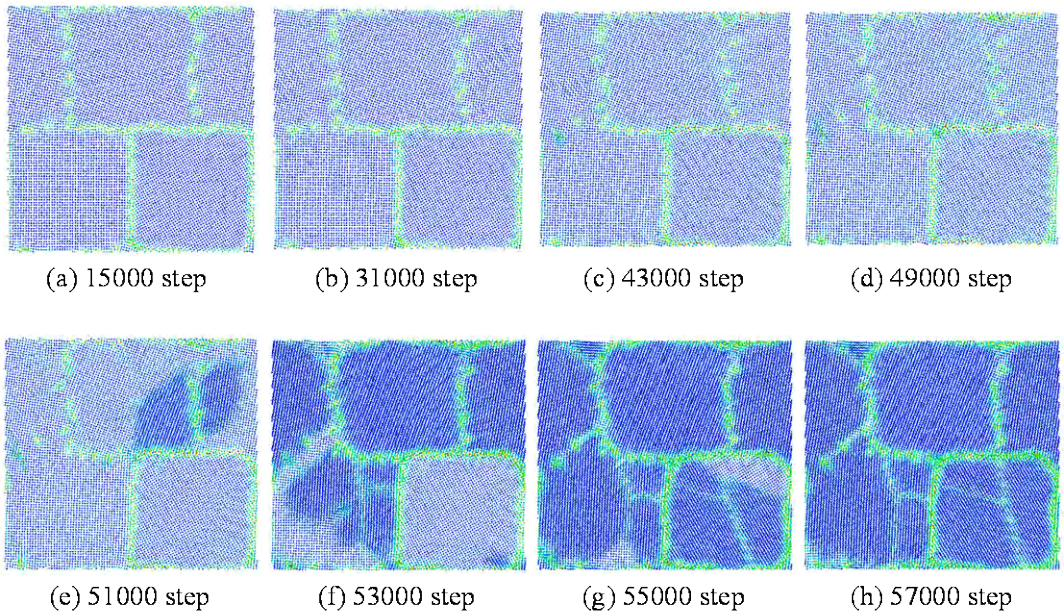

Fig. 2. Variation of the configuration of atoms for Model Az1. The color indicates the potential energy of each atom.

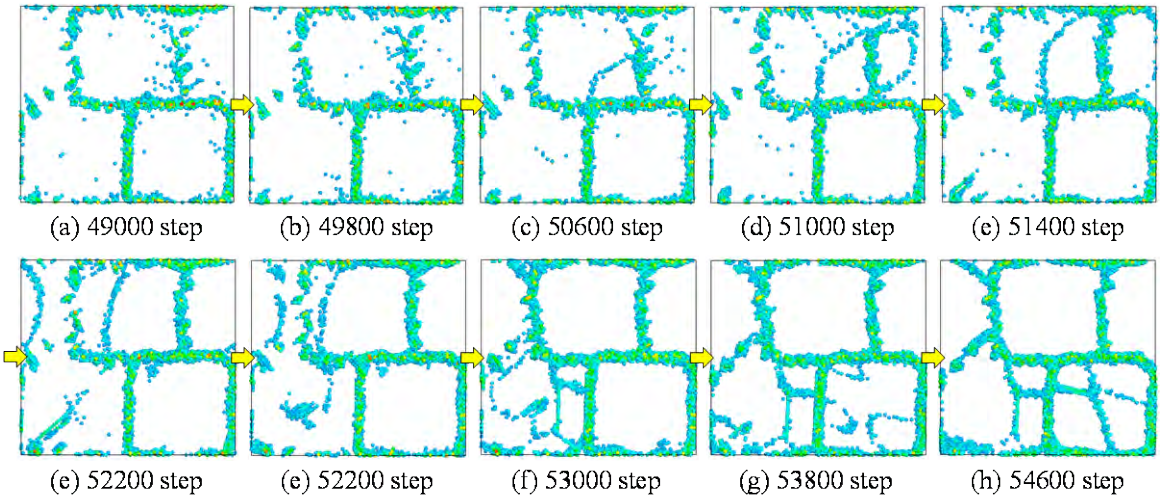

Fig. 3. Variation of atomic configuration in the duration of initiation of the plastic deformation for Model Az1. Only the atoms having potential energy valued higher than a certain threshold, here ϕ = -7.8.

crystal structure is observed until the 49000th time step, while slight variations are observed in the grain boundaries. Subsequently, an apparent change is observed at the 51000th time step, as shown in Fig. 2(e): an area depicted in dense blue color appears around the top-right area. This is caused by the change in the crystal orientation in the depth direction; the [001] direction completely accorded with the *z*-axis originally, but the orientation shifted slightly and the atoms in the depth direction become visible. It is also notable that this area is centered at a grain boundary, and spread across two grains. This area extends quickly over Grains 3 and 4. A new dense-blue area is also generated in Grain 1 by the 53000th time step. Subsequently, similar change appeared in Grain 2, and finally a series of the change complete by the 57000th time step.

To see the phenomena occurring more clearly, only the atoms at unstable state are made visible and displayed at short intervals between the 49000 and 55000th time steps in Fig. 3. Values in the potential energy are taken as the indicator of the instability, and the threshold value is chosen as -7.8. Most unstable atoms are located on the grain boundaries except for

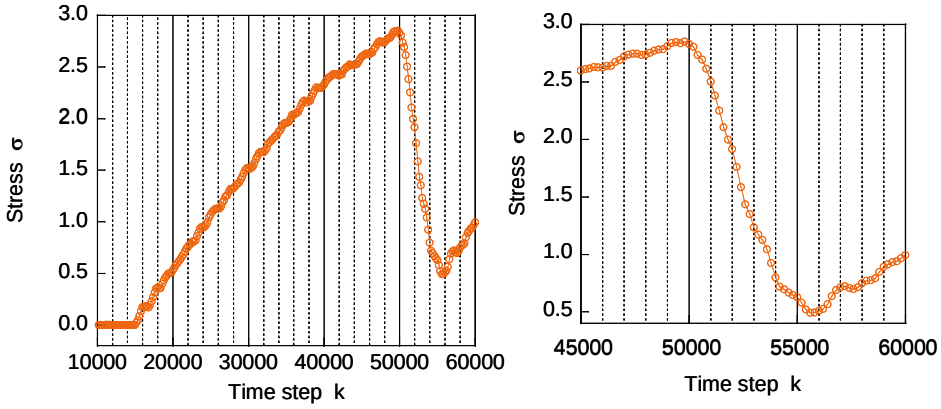

Fig. 4. Variation of stress in the *y* direction for Model Az1. (a) Overall view from the beginning of loading and until the end of yielding. (b) Magnified view around the yielding.

several atoms scattered inner grains at the 49000th and 49800th time steps. Then a linear defect appears in the top-center grain (Grain 3) at the 50600th time step, and the defect spread in Grain 3. Compared with Fig. 2 (e) and Figs. 3 (c) and (d), the apparent linear defect in Fig. 3 corresponds to the boundary of the dense-blue area in Fig. 2, and actually the defect is planer one. In addition, the origin of the defect is the right-bottom corner of the grain, or the triple junction of the grains, and the transformed area spread in Grain 3. Then the transformed area crosses over the grain boundary and extended in Grain 4.

The variation in the compressive stress is shown in Fig. 4. The stress increases monotonously as compressive load is imposed from the 15000th time step. Then the stress decreases abruptly at the 50000th time step. The peak point is very sharp, but the decrease is not momentary; it takes about 5000 time steps until the stress reaches the bottom. The initiation of the defects was determined from Fig. 3 to be the 50000th time step, which clearly corresponds to the peak in Fig. 4. Additionally, it is also confirmed that the duration of the expansion of the deformed area corresponds well to the duration of the stress decrease, from the 50000th to 55000th time step. Therefore, it can be considered that yielding occurred in this duration.

Simulation Results --- Other Cases

Simulation results for all cases are shown in Fig. 5. Variations in the stress show similar tendency; the stress increases monotonously and decreases drastically at around the 50000th time step. The peak values in stress are different for every case; minimum $\sigma = 2.5$ for Model Bz1, and maximum $\sigma = 3.1$ for Model Az3. The reduction depth and duration spent for the stress drop are approximately the same. An overall tendency that Models A exhibits higher peak than Models B can be seen, though more data is necessary for draw a conclusion. Another interesting feature is that some cases, for example Models Az2 and Bz1, show some plateau duration around the peak. Figure 5 (b) shows the configuration of unstable atoms just after the stress peak for some typical cases. Common to Models Az2 and Bz1 both of which exhibit a plateau around the stress peak, a straight line defect is generated, as shown in Figs 5(b)(i) and (iii). In other cases for which a sharp peak is observed, in contrast, a

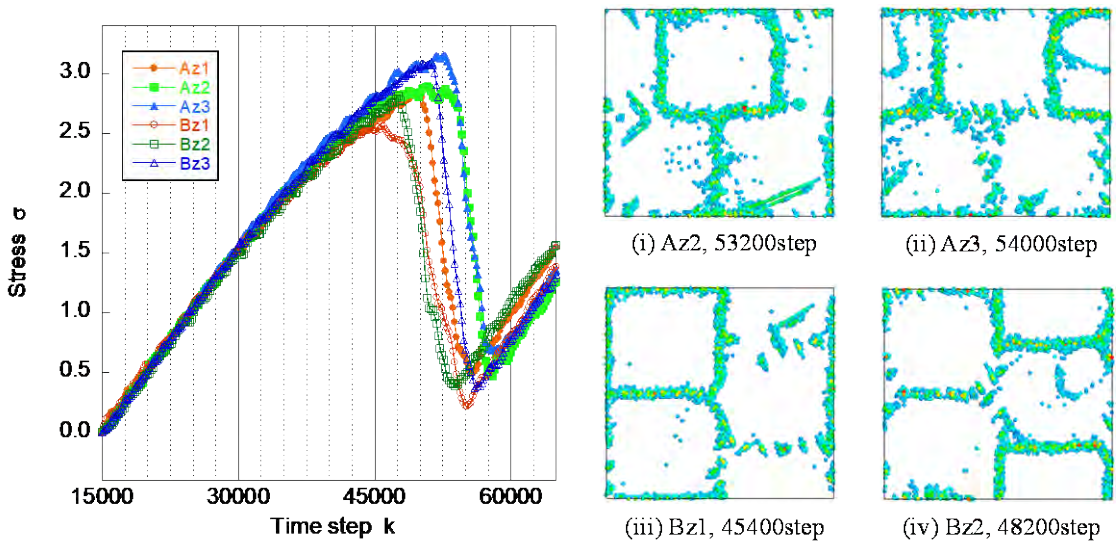

(a) (b)

Fig. 5. Variation in stress for all models (a), and the configuration of unstable atoms around the initiation of the plastic deformation for some typical cases (b).

transformation domain surrounded by curved defects are generated, as shown in Figs 5(b)(ii) and (iv) for Az3 and Bz2 as well as Fig. 3(c) for Az1. These defects correspond to planer defects as can be seen in Fig. 2(e). The cause of generation of different type of defects, linear or planar ones, is inferred to be the structure of grain boundary, since the origins of both types of defects are considered to be on the grain boundaries. Additionally, the crystal orientation of the grains in which linear defects are generated, i.e. Grain 2 in Model Az2 and Grain 4 in Model Bz1, is commonly -20 deg., as listed in Table 1. The orientation with respect to the external load is also one of the key factors dominating the behavior, which will be discussed in our future work in detail.

Conclusion

Molecular dynamics simulations were carried out to investigate the initiation mechanism of plastic deformation in a nanocrystalline material. Two types of simple models having four grains with different arrangements were prepared, and a uniaxial compression was imposed. Simulations were carried out varying the combination of the crystal orientations of every grain. As a result, the following results were obtained. Common to all models, the stress increased monotonously, when the grain sustains the initial configuration. Then, an abrupt drop in stress was observed. At this moment, a linear or planar defect was generated, and this is considered the initiation of the plastic deformation. The defects spread in a certain time duration, which is considered as yielding. Further investigation is still required for clarifying the mechanism in more detail. Full three-dimensional model is necessary to simulate slip phenomena on the (111) plane. Application of more precise inter-atomic potential is required not only for quantitative evaluation but also for distinguishing some more delicate mechanism. However, it revealed that fundamental insights can be derived using the present model, and further investigation is now in progress.

References

[1] Segal, V.M. (1999) Equal channel angular extrusion: from macromechanics to structure formation. *Materials Science*, **54**, 427-510.

[2] Saito, Y., Utsunomiya, H., Tsuji, N. and Sakai, T. (1999) Novel ultra-high straining process for bulk materials --- Development of the accumulative roll-bonding (ARB) process. *Acta Materialia*. **47**, 579-583.

[3] Sidor, J., Miroux, A., Petrov, R. and Kestens, L. (2008) Microstructural and crystallographic aspects of conventional and asymmetric rolling processes. *Acta Materialia*, **56**, 2495-2507.

[4] Van Swygenhoven, H., Caro, A. and Farkas, D. (2001) A molecular dynamics study of polycrystalline fcc metals at the nanoscale: grain boundary structure and its influence on plastic deformation. *Materials Science and Engineering A*, **309**-**310**, 440-444.

[5] Trautt, Z.T. and Mishin, Y. (2012) Grain boundary migration and grain rotation studied by molecular dynamics. *Acta Materialia*, **60**, 2407-2424.

[6] Spearot, D.E. and Sangid, M.D. (2014) Insights on slip transmission at grain boundaries from atomistic simulations. *Current Opinion in Solid State and Materials Science*, **18**, 188-195.

[7] Uehara, T., Wakabayashi, N., Hirabayashi, Y. and Ohno, N. (2008) An atomistic study of grain boundary stability and crystal rearrangement using molecular dynamics techniques. *International Journal of Mechanical Sciences*, **50**, 956-965.

[8] Uehara, T., Asai, C. and Ohno, N. (2009) Molecular dynamics simulation of shape-memory behaviour using a multi-grain model. *Modelling and Simulation in Materials Science and Engineering*, **17**, 035011.

[9] Uehara, T. (2015) Molecular dynamics simulation on transformation-induced plastic deformation using a Lennard-Jones model. *Key Engineering Materials*, **626**, 414-419.

[10] Uehara, T. (2017) Molecular dynamics simulation of the variation in the microstructure of a polycrystalline material under tensile load. *Key Engineering Materials*, **748**, 375-380.

[11] Uehara, T. (2017) Molecular dynamics simulation of microstructural change in a poly-crystalline FCC metal under compression. *Proceedings of XIV Int. Conf. on Computational Plasticity*, 106-113.

[12] Uehara, T. (2017) Molecular dynamics simulation of grain refinement in a polycrystalline material under severe compressive deformation, *Materials Sciences and Applications*, **8**, 918-932.